

pubs.acs.org/Macromolecules Article

Cascade Ring Strain Release Polymerization of Cyclohexene Oxide and Derivatives Using a Mono(μ -Alkoxo)bis(alkylaluminum) Initiator

Benjamin J. Pedretti, Congzhi Zhu, Hironobu Watanabe, Sadahito Aoshima, and Nathaniel A. Lynd*



Cite This: *Macromolecules* 2023, 56, 4884–4894



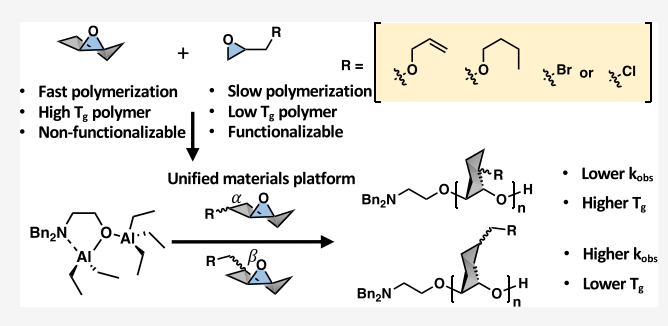
ACCESS

III Metrics & More

Article Recommendations

s Supporting Information

ABSTRACT: Cyclohexene oxide (CHO) is a useful building block for the synthesis of novel materials and is a model substrate for polymerization catalyst development. The driving force for CHO polymerization is derived from its bicyclic structure, which combines the release of the enthalpy from epoxide ring-opening (ca. –15 kcal/mol) and a twist-chair-to-chair conformation shift in the cyclohexane ring (ca. –5 kcal/mol) upon enchainment. The lack of regio-defined functional handles attached to the CHO monomer limits the ability to both pre- and post-functionalize the resultant materials and establish structure—property relationships, which reduces the versatility of currently accessible materials. We



report the synthesis of two series of CHO derivatives with butyl, allyl, and halogen substituents in the α and β positions relative to the epoxide ring. Adding substituents to the CHO ring was found to affect polymerization kinetics, with 4-substituted (β) CHO being more reactive than 3-substituted (α) CHO analogs when initiated with a mono(μ -alkoxo)bis(alkylaluminum) pre-catalyst. Polymer thermal properties depended on substituent location and identity. Halogenated CHO rings were most reactive and produced the highest glass transition temperatures in the resultant polymers (up to 105 °C). Density functional theory revealed a possible mechanistic explanation consistent with the observed differences in polymerization rate for the 3- and 4-substituted CHOs derived from a combination of steric and thermodynamic considerations.

INTRODUCTION

Epoxides are useful precursors and intermediates for smallmolecule synthesis 1-3 and as building blocks for polyethers, 4-6 polycarbonates, 7,8 and other heteropolymers. Polyetherderived materials represent a highly versatile materials platform with excellent modularity for compositional control and the tuning of structure—property relationships. 10-15 The versatile nature of these materials is derived from the wide variety of available epoxide monomers 11,16 and the ease with which many polymers can be post-functionalized. 10,17 High reaction rates are typical for epoxides because of the substantial enthalpic driving force for epoxide ring-opening. 18 Homopolymers, statistical copolymers, and block polymers have all been synthesized from different functionalized epoxides using anionic, 5,17,19 cationic, 20–22 and catalytic approaches. 6,16,23–26 Additionally, polyethers have been used in a wide variety of applications as components in elastomers, polyurethanes, resins, and a variety of other materials on commercial scales. 27-30 The decades-long industrial production of elastomers such as poly[(epichlorohydrin)-co-(allyl glycidyl ether)-co-(ethylene oxide)] is accomplished using the Vandenberg catalyst.4,31,32

The aluminum chelate catalyst, introduced by Vandenberg, led to a series of classical studies of the stereochemistry of polymers synthesized from disubstituted epoxides including cyclohexene oxide (CHO) and *cis-* and *trans-*butene

oxide.31,33,34 Renewed interest in the stereochemistry of CHO polymerizations with zinc-based chiral and achiral catalysts has led to a better mechanistic understanding of disubstituted epoxide polymerization. 35,36 Using the highly versatile Vandenberg catalyst as inspiration, our group serendipitously discovered a new organoaluminum-based initiator system for the ring-opening polymerization of epoxides; the mono(μ -alkoxo)bis(alkylaluminum)s (MOBs).²⁴ The MOB system initiates a reasonably controlled polymerization with improved tolerance for monomer functionality over traditional anionic ring-opening polymerization. 16 Molecular weight control and functional group tolerance make this system well-suited for producing previously inaccessible compositions and architectures. Despite the functional group tolerance these catalysts and other catalytic systems have demonstrated, most materials development efforts use terminal epoxides such as ethylene oxide, alkylene oxides, or derivatives of epichlorohydrin such as the

Received: March 14, 2023 Revised: May 1, 2023 Published: June 30, 2023





glycidyl ethers. 11,16,37 The scope of typical monomers is due to the availability of the alkylene oxides and the ease with which epichlorohydrin may be used to glycidylate nearly any alcohol under mild reaction conditions. An alternative monomer platform based on, for example, a highly strained CHO could increase polymerization rates relative to terminal epoxides, increase glass-transition temperature $(T_{\rm g})$ of the resulting polymers, and expand the scope of new polyether materials.

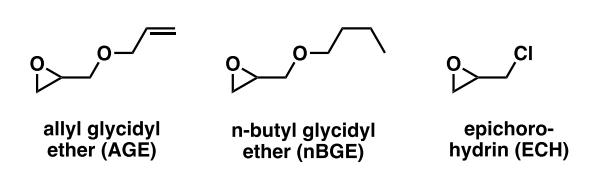
Research involving CHO has mainly focused on understanding its copolymerization with CO₂, ³⁹⁻⁴⁷ lactides, ⁴⁸⁻⁵⁰ and anhydrides 51-56 to form degradable polyesters and polycarbonates. For example, Williams and co-workers have developed efficient catalysts for CHO-containing copolymerizations and expanded the library of accessible materials from renewable resources, ^{39–42,56,57} while Diaconescu and coworkers have developed redox-switchable catalysts for the synthesis of polyCHO-b-polyesters. $^{58-61}$ Others have used CHO and other epoxides to synthesize bicyclic lactones that can be polymerized into degradable, recyclable poly(ether ester)s. 62-64 An attractive feature of poly(cylcohexene oxide)based degradable polyesters and polycarbonates is the facile regeneration of the monomers post-degradation.⁶⁵ Williams and co-workers recently reported on the recyclability of poly(cyclohexene carbonate) back to the CHO monomer using a bimetallic Mg^{II} catalyst with yields up to 98%.⁶⁶ This work highlighted that CHO-containing polymers may be ideal candidates for further investigation as replacements for commonly used, petroleum-based polymers because of their ease of chemical recyclability back to monomers compared to other epoxide-containing polymers. The chemical recycling strategy allows for recycling and regeneration of materials with properties identical to the virgin plastic.

In the development of new catalytic systems for polyether synthesis, CHO has been used as a model substrate in part because of its high reactivity relative to other epoxides.⁶⁷ Although PCHO is one of the few examples of a moderately high T_{σ} (>50 °C) polyether synthesized in a chain-growth polymerization, the lack of CHO derivatives limits the versatility of resultant materials. Functionalized CHO-derivatives would produce a new class of polyethers with a more rigid PCHO backbone instead of the flexible [-CH2-CH(R)- $O-]_n$ backbone derived from terminal epoxides. Derivatives of CHO with reactive pendant groups could be functionalized after polymerization to produce a variety of different polymers with tunable properties. Copolymerization of CHO with CHO derivatives could be used as a strategy to modulate bulk polymer characteristics such as $T_{\rm g}$ and mechanical toughness. Schneiderman et al. studied the effects of adding n-alkyl substituents to δ -valerolactone on both the polymerization rate as well as the physical properties of the resulting polymers, 70 yet this type of study has not been used on CHO-based epoxide monomers. Finally, although CHO is frequently used as a substrate in catalyst development, little work has been done on understanding the basis for CHO's significantly higher reactivity compared to many terminal epoxides.⁷

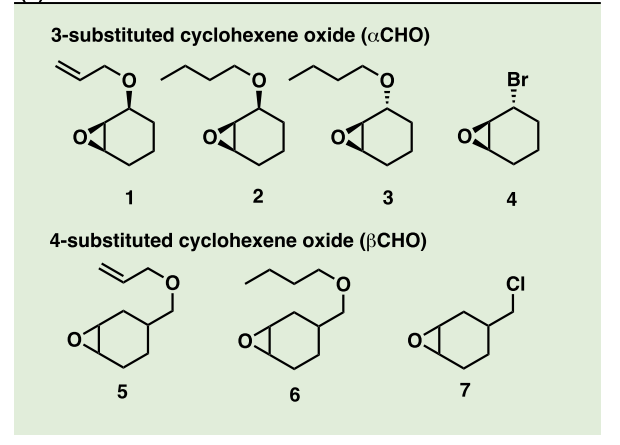
In this report, we investigate the molecular basis for the high reactivity of CHO by synthesizing structures analogous to common terminal epoxide monomers to understand the interplay between the added substituents and the reactivity of the bicyclic monomer (Scheme 1a,b). CHO derivatives with butyl, allyl, and halogen substituents were synthesized at both the α (α CHO series) and β (β CHO series) positions relative to the epoxide ring (Scheme 1b). Polymerization rates were

Scheme 1. (a) Conventional Epoxide Monomers. (b) Range of Novel Monomers Investigated in This Study

(a) Example conventional epoxide monomers



(b) New monomers in this work



significantly impacted by the size and relative stereochemistry of substituents for the α CHO series when using the MOBbased initiator system. The reactivity of the β CHO series monomers, in contrast, had similar polymerization rates to unsubstituted CHO. Computational studies using density functional theory (DFT) were conducted to better understand the differences in reactivity we observed between the two sets of CHO monomers, mono-substituted epoxides, and CHO. 42,50,71 The effect of the substituents on both the steric and electronic environments of the reactive sites provided an explanation for the different reactivities of the monomers. DFT results additionally supported a possible mechanism for the polymerization and offered insights into the higher polymerization rate of CHO over monocyclic epoxide monomers, which were related to a cascade of ring strain release of both epoxide and a conformation shift of the cyclohexane ring from an unstable twist chair to a more stable chair conformation. Finally, a regiochemical analysis using ¹³C NMR spectroscopy showed that substituted CHO monomers were incorporated into polymer chains with little regularity in tacticity, similar to PCHO made with other achiral catalysts.^{36,72}

■ RESULTS AND DISCUSSION

Monomer Synthesis. Two series of substituted CHOs were synthesized (Scheme 2). The α CHO series was synthesized with the substituent α to the epoxide starting with either cyclohexenone or 3-bromocyclohexene, whereas β CHO series was synthesized with the substituent β to the epoxide starting with 3-cyclohexene-1-carboxaldehyde. Because most commercially available substituted epoxides are typically sold as a mixture of enantiomers, both series were made using reactions that are not enantioselective. To make a large library of materials accessible without significant synthetic burden, we used a minimal number of high-yielding, orthogonal reactions as shown in the Supporting Information. Carbonyl reduction with sodium borohydride followed by epoxidation with m-

Scheme 2. (a) MOB-Initiated Polymerization of High-Strain CHO Monomers to Produce Poly(cyclohexene oxide) Derivatives; (b) Pre-catalyst Structure and Functional Groups of Novel CHO Derivatives

(a) Cascade ring strain release polymerization

(b) MOB structure and monomer functional groups

$$MOB = Bn_2N \underbrace{Al}_{O-Al} \underbrace{Al$$

chloroperoxybenzoic acid (mCPBA) afforded the precursor epoxy alcohols (Compounds 9 and 12) to cis-allyloxy- α CHO, cis-butoxy- α CHO, as well as allyloxy- β CHO and butoxy- β CHO. Purification by column chromatography after the second step produced Compounds 9 and 12 in overall yields as high as ca. 66%. Because mCPBA epoxidation has low atom efficiency and the resulting product is too hydrophilic for extraction to be efficient, the challenging removal of the m-chlorobenzoic acid byproduct decreased the overall yield of the pure product.

The hydroxyl group of 2-cyclohexenol directed epoxidation by mCPBA to the same side of the ring as the hydroxyl group through the formation of an intra-molecular hydrogen bond, allowing for the synthesis of the cis- α CHO monomers.⁷³ The two epoxy alcohols were treated with sodium hydride and either allyl bromide or 1-bromobutane for the final Williamson etherification step to yield the desired monomers. For transbutoxy- α CHO, the carbonyl reduction was followed by Williamson etherification to create a cyclohexene-butyl ether. mCPBA epoxidation without a directing group then yielded the epoxide in an anti-facial position relative to the butoxy group as the epoxidation favors the less sterically hindered face of the alkene. This strategy was also employed for the synthesis of trans-bromo- α CHO through the mCPBA epoxidation of 3bromocyclohexene. For the α CHO series, column chromatography removed the undesired diastereomers. For chloro- β CHO, a modified Appel reaction⁷⁴ was employed, starting with 3-cyclohexene-1-methanol to afford the corresponding alkyl halide. Epoxidation with mCPBA was then used to produce the monomer.

Kinetics Studies and Comparison to Terminal Epoxide Polymerizations. All monomers were polymerized

Table 1. Summary of $Bn_2N(CH_2)_2(\mu_2-O)Al(Et)_2\cdot Al(Et)_3$ -Initiated Polymerizations^a

monomer	target $M_{\rm n}$ (kg/mol)	$M_{\rm n}^{b}$ (kg/mol)	$M_{\rm n}^{\ c}$ (kg/mol)	Ð	conversion after 5 min (%)	conversion after 24 h (%)	$T_{\rm g}$ (°C)
AGE	9.1	7.1	5.3	1.54	10	77	-79
AGE	9.1	6.7	5.0	1.44	10	77	-76
nBGE	10.4	7.9	4.2	1.31	16	78	-80
nBGE	10.4	7.8	4.0	1.34	17	77	-80
ECH	7.4	6.9	7.0	1.38	29	>99	-49
ECH	7.4	7.1	7.9	1.23	29	>99	-45
СНО	7.9	6.5	10.9	2.33	87	97	58
СНО	7.9	5.8	8.2	2.96	85	96	57
cis-allyloxy- $lpha$ CHO	12.3	9.4	19.6	1.94	57	85	23
cis-allyloxy- $lpha$ CHO	12.3	10.3	16.2	1.87	59	86	22
cis-butoxy- $lpha$ CHO	13.6	19.6	17.7	2.04	49	82	16
cis-butoxy- $lpha$ CHO	13.6	20.0	14.1	2.23	49	84	15
trans-butoxy- $lpha$ CHO	13.6	14.0	10.1	2.07	11	91	37
$\textit{trans} ext{-butoxy-}\alpha\text{CHO}$	13.6	16.0	9.3	1.90	15	84	33
trans-bromo- $lpha$ CHO	14.2	6.1	1.6	2.80	90	95	105
trans-bromo- $lpha$ CHO	14.2	3.0	0.8	2.66	90	96	101
allyloxy- β CHO	13.5	13.8	11.2	1.44	76	>99	-11
allyloxy- β CHO	13.5	13.3	9.1	1.46	69	>99	-11
butoxy- β CHO	14.7	22.1	14.2	2.43	78	96	-16
butoxy- β CHO	14.7	22.5	12.9	2.42	59	87	-17
chloro- β CHO	11.7	10.0	18.7	3.64	66	94	83
chloro- β CHO	11.7	10.1	12.2	3.22	76	92	82

[&]quot;Reactions were run neat at 60 °C for 24 h. "Molecular weight determined by end group analysis in ¹H NMR spectra using either the dibenzyl end group protons or reacting the terminal hydroxyl group with trichloroacetyl isocyanate to extract the terminal methine proton signal. ⁷⁵ "Molecular weight determined by SEC relative to polystyrene standards. All polymerizations were done with $[M]_0/[I]_0 = 80$. Each polymerization was run in duplicate.

under identical, neat conditions in an inert glove box utilizing the pre-catalyst shown in Scheme 2b. The mono(μ -alkoxo)bis(alkylaluminum) (MOB) initiator system was used for this study because it has been shown to polymerize a variety of terminal epoxides with broad functional group tolerance. 16 All polymerizations were run at 60 °C. Although it would be ideal to conduct the polymerizations above the glass transition temperatures of all of the resultant polymers, alkyl aluminum decomposition would occur at higher temperatures (ca. 100 °C). A summary of the outcomes of the polymerizations is presented in Table 1. The initial monomer/initiator ratio was kept constant at 80:1 by mole, targeting polymers with molecular weights between 7.4 and 14.7 kg/mol. For these experiments, the least-active MOB initiator previously reported, $Bn_2N(CH_2)_2(\mu_2-O)Al(Et)_2 \cdot Al(Et)_3$, was chosen because of the high reactivity of CHO and because the reaction kinetics of a slower polymerization are more easily monitored.

As shown in Table 1, the polymerizations of terminal epoxide monomers exhibited control over molecular weight (M_n) and dispersity (D), though allyl glycidyl ether (AGE) and n-butyl glycidyl ether (nBGE) had lower conversions at 24 h than epichlorohydrin (ECH). Additionally, all three of the monosubstituted polyethers remained as viscous liquids and were able to stir throughout the polymerization, which is typical for low $T_{\rm g}$ polyethers.³⁷ The first polymerizations of CHO initiated by ${\rm Bn_2N(CH_2)_2}(\mu_2\text{-O}){\rm Al(Et)_2}\cdot{\rm Al(Et)_3}$ were more rapid and less controlled. A reaction exotherm was observed under both neat and diluted conditions (3:1 toluene/ CHO by volume) at the start of the polymerizations, likely due to the rapid release of ring strain enthalpy. In the case of the neat polymerization, the temperature of the reaction increased from room temperature to a high of ca. 86 °C in the first minute of polymerization. The addition of solvent slowed the reaction and lowered the adiabatic temperature increase to ca. 59 °C in the case of the 3:1 dilution with toluene; however, the addition of solvent did not lead to improved polymer characteristics such as a lower dispersity and instead only decreased conversion. For reference, the polymerization of both AGE and nBGE resulted in initial temperature increases to ca. 35-36 °C in the first minute of polymerization. Nonisothermal, neat polymerization conditions were used for all α CHO and β CHO derivatives. Due to the non-isothermal nature of the polymerization of the most active CHO monomers, reaction rate constants are not easily compared. The conversion of monomer to polymer after 5 min is instead used as a comparison of relative initial polymerization rates. Most of the resultant polymers had glass-transition temperatures below the reaction temperature. Polymerization conversion was measured by ¹H NMR spectroscopy of timepoint aliquots as shown in Figure 1 for *cis*-butoxy- α CHO. The two epoxide peaks located between 3.20 and 3.30 ppm give way to the broad polymer backbone ether peaks at ca. 3.40-3.50 ppm. The time-dependent conversation data are presented in Figure 2 as polymerization conversion versus time for the substituted CHOs and compared with the terminal epoxide analogues.

As can be seen in Figure 2a, nBGE, AGE, and ECH exhibited behavior typical in a MOB-initiated polymerization with ECH polymerizing more quickly than the glycidyl ethers. ²⁴ CHO exhibited the fastest polymerization rate of the four commercially available monomers (Figure 2a), reaching ca. 85% conversion after just 5 min. After this time, the polymerization rate drops to nearly zero as the system

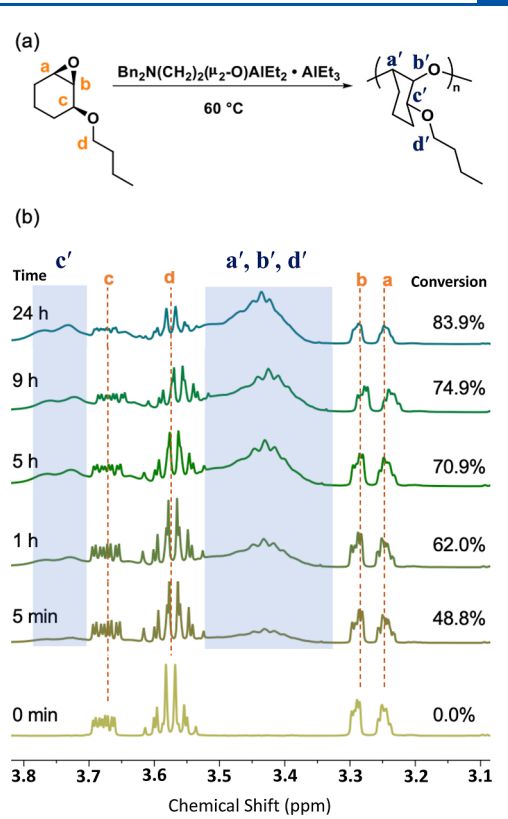


Figure 1. (a) Polymerization of *cis*-butoxy- α CHO and (b) 1 H NMR spectroscopy (500 MHz, CDCl₃) throughout the course of the polymerization. Epoxide peaks located between 3.20 and 3.30 ppm give way to the broad polymer backbone ether signals located at ca. 3.40–3.50 ppm.

becomes glassy due to the rising $T_{\rm g}$ of the resulting PCHO ($T_{\rm g} \approx 57{-}58~^{\circ}{\rm C}$) in the reaction mixture. The polymerization continued over the course of the next 24 h; however, the rate was presumably limited by the diffusion of monomer to active chain ends.

Comparing Figure 2a to the α CHO series in Figure 2b, trans-bromo-αCHO had similar reaction kinetics to CHO itself. Although all monomers, including CHO, exhibited an adiabatic temperature increase at the start of the polymerization, the temperature increase of trans-bromo- α CHO was most comparable to CHO itself and the reaction reached ca. 90% conversion after just 5 min. The reaction became glassy after a few minutes, causing the reaction rate to decrease and the conversion to remain nearly constant for the remainder of the experiment. Analysis of the final product revealed that although the monomer was quickly converted to polymer, the resultant molecular weights were lower than expected. We believe that the initial exotherm may have caused some of the MOB pre-catalyst to decompose, leading to parasitic initiation, as well as some of the monomer to decompose via elimination of HBr to create a CHO monomer with a carbon-carbon double bond adjacent to the epoxide ring. The appearance of peaks at 5.5-6.0 ppm in the polymer ¹H NMR spectrum (Figure S52) indicates that early termination may have occurred in this reaction via an elimination or transfer reaction. Additionally, MALDI mass spectrometry revealed signals consistent with the presence of polymers that contain monomers that decomposed to the alkene and polymers not initiated by the pre-catalyst (Figure S71), further supporting the theory of HBr loss and initiator decomposition. These

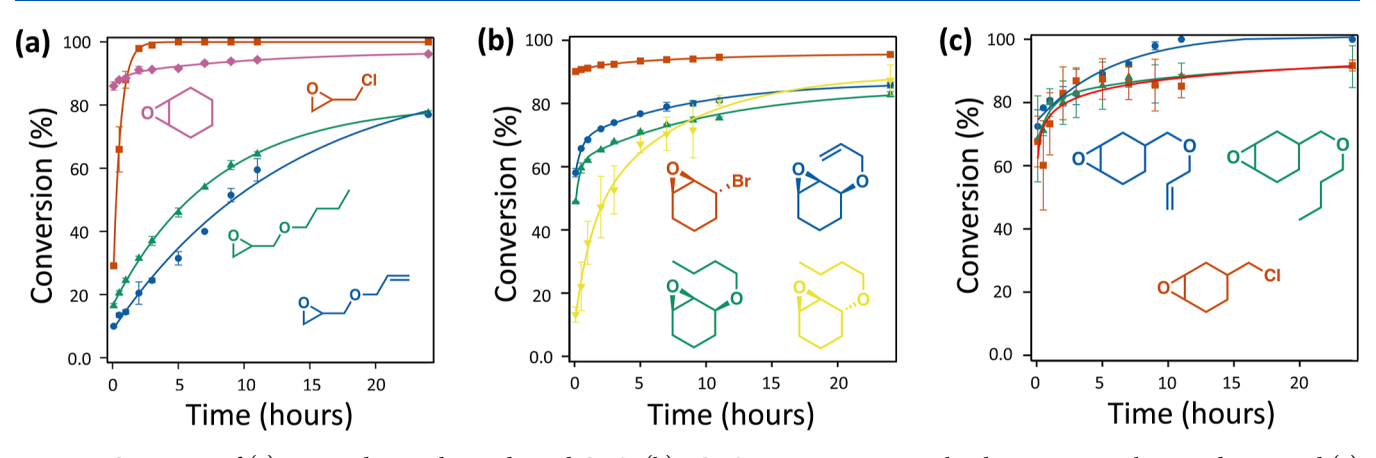


Figure 2. Conversion of (a) mono-substituted epoxides and CHO, (b) α CHO series monomers with substituents α to the epoxide ring, and (c) β CHO series monomers with the substituent β to the epoxide ring. Trials were run in duplicate under the same neat conditions at 60 °C over the course of 24 h targeting an initial monomer/initiator ratio of 80. Conversion was monitored over time with ¹H NMR spectroscopy (400 MHz, CDCl₃).

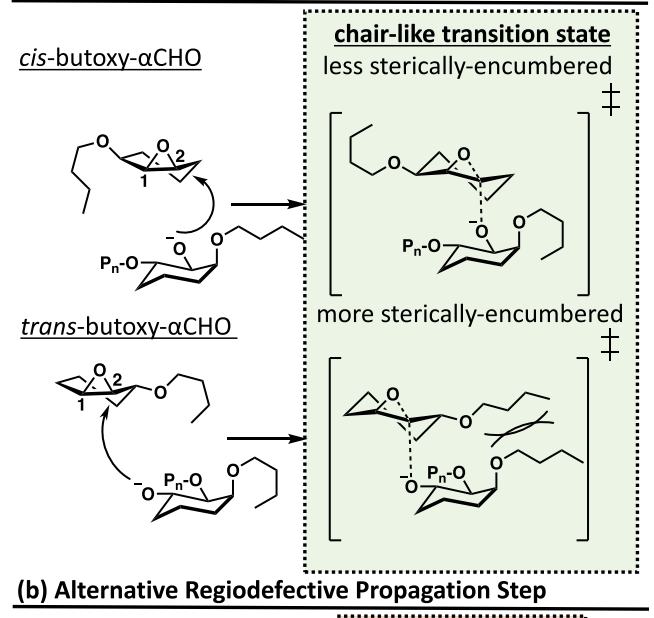
undesired reactions that may have been caused by the initial reaction exotherms may have contributed to the broader molecular weight distributions of PCHOs relative to other polyethers synthesized with the MOB pre-catalyst.

cis-Allyloxy- α CHO and cis-butoxy- α CHO demonstrated similar reaction kinetics, with the polymerization of cisallyloxy- α CHO proceeding faster than cis-butoxy- α CHO. Both monomers were synthesized such that the predominant set of diastereomers have the epoxide cis to the substituent. With the substituent groups facing the same side as the epoxide ring, it is plausible that the larger substituent would increase steric congestion near the epoxide and slow the reaction relative to a monomer with a smaller substituent.

The α CHOs and monosubstituted epoxides display substituent groups directly adjacent to the epoxide ring, yet the rates of polymerization of cis-allyloxy- α CHO and cisbutoxy- α CHO were initially faster than the polymerization of the analogous glycidyl ethers AGE and nBGE, which exhibit the same through-bond separation between epoxide and ether substituent. The difference in polymerization rate was likely caused by two factors that will be explored further in the computational section of this article. Significantly, CHO in a twist-chair configuration contains more ring strain and, therefore, has a larger thermodynamic driving force than the epoxide moiety of the glycidyl ethers alone. This added ring strain also leads to a larger release of energy upon monomer enchainment, leading to more significant adiabatic temperature increases, which further increases the polymerization rate. Additionally, in the case of the terminal epoxides (AGE, nBGE, and ECH), the substituents have more conformational freedom and can sterically encumber the epoxide group. cis-Allyloxy- α CHO and *cis*-butoxy- α CHO have their substituent groups locked in a position pointing away from the electrophilic carbon atoms of the epoxide (see Figure 3a), leaving carbon atoms 1 and 2 of the epoxide more exposed to reactive polymer chain ends.

While both cis- α CHO monomers polymerized faster than their analogous monosubstituted epoxides, the β CHO analogues polymerized at a higher initial rate than the α CHO monomers (Figure 2c), reaching ca. 70% conversion in 5 min. With the substituents placed β to the epoxide, the reactivity was similar for all three monomers for the first 5 h of polymerization. With the substituents farther from the reactive

(a) Simplified Propagation Step (Lowest Energy)



R' = butoxy group for *cis*-butyl CHO R'' = butoxy group for *trans*-butyl CHO

Figure 3. (a) Simplified propagation step for the polymerization of the α CHO cis- and trans-butyl CHO monomers. In both cases, the lowest energy intermediate forms from attack at carbon 2, which yields the 1,2-trans diaxial product. (b) Attack at carbon 1 is less favorable but is still accessible. Alkyl aluminum species not shown for clarity.

center, steric hindrance from the substituents was less significant. Furthermore, the relative stereochemistry of the substituent to the epoxide is expected to have a reduced effect when further away from the epoxide ring. These conclusions were consistent with the proposed anionic-type polymerization

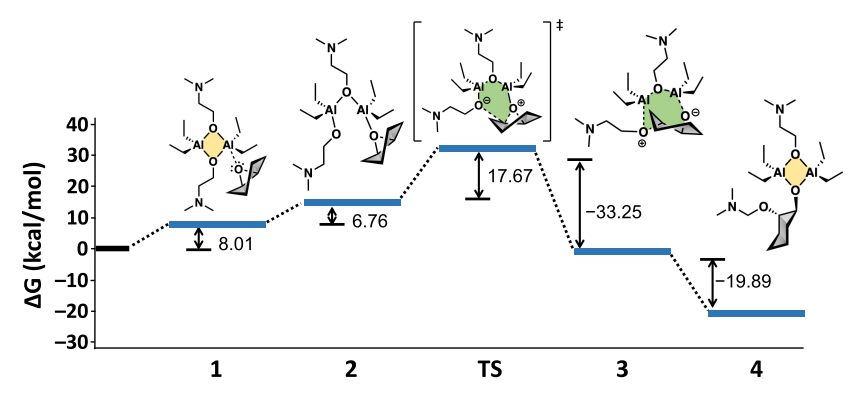


Figure 4. Relative energies of proposed intermediates for the initiation of CHO polymerization with a bis-aluminum complex. For clarity, the benzyl groups on the amine have been replaced with methyl groups and the trialkyl aluminum adducts with the amines are omitted.

mechanism. With the substituent further away from the epoxide, the electrophilic carbon atoms of the CHO ring were sterically more accessible to the propagating center of the polymerization. Additionally, the alkoxide resulting from the epoxide ring opening was less sterically encumbered and, therefore, more reactive in the propagation step. After the first few hours of the polymerization, all β CHO monomer polymerization rates likely became diffusion limited.

cis-Butoxy- α CHO, with butoxy and epoxide groups cis to each other, reacted faster than trans-butoxy- α CHO with the substituent and epoxide opposite to each other. This result may seem counterintuitive based on a steric argument for the propagation steps. If the epoxide ring is on the same side of the cyclohexane ring as the substituent and is opened, the propagating alkoxide would be sterically encumbered by the butyl substituent, making it more difficult for the alkoxide to react with another epoxide. However, when the three-dimensional structure of the monomers is considered (Figure 3), a plausible reason for this result can be elucidated.

For both the *cis*- and the *trans*-butoxy- α CHOs, the lowest energy propagation step should involve the propagating alkoxide attacking the next epoxide in a pre-axial orientation to proceed through a more stable chair-like transition state (TS) (Figure 3a), consistent with the Fürst-Plattner Rule, resulting in an opened ring with the new ether oxygen and alkoxide in a *trans* diaxial orientation. This behavior has been well-studied and documented for the ring opening of CHO and CHO derivatives with a variety of nucleophiles and under both catalyzed and uncatalyzed conditions. 71,77-81 This pathway is only possible if the attack happens at carbon 2 of the epoxide, as shown in Figure 3a. Attack at this carbon for both cis and trans monomers is favored because the C2-O bond is longer and, therefore, more easily broken than the C_1 -O bond after both monomers coordinate to the aluminum (see Table S2 in the Supporting Information). We hypothesize that the attack at carbon 2 is faster in the case of *cis*-butoxy- α CHO because this carbon atom is farther away from the bulky butoxy group than it is from trans-butoxy- α CHOs. The butoxy group in trans-butoxy- α CHOs is also on the same face of the cyclohexane ring as the alkoxide attack is, increasing the steric hindrance around the electrophilic carbon atom and slowing polymerization. Because this polymerization is believed to proceed through an anionic-type coordination mechanism, the propagation step is steric approach-controlled. Hansen and coworkers have previously explored the Lewis acid-catalyzed ring opening of CHO at both carbon atoms and found that ring opening through a chair-like TS had a lower energy barrier

than the twist—boat TS regardless of the Lewis acid.⁷¹ The reaction of either monomer proceeding through an attack on carbon 1 is less energetically favorable due to the twist boat TS (Figure 3b); however, it is still possible if the more favorable carbon is less sterically accessible.

The overall polymerization conversions of *cis*- and *trans*-butoxy- α CHO converge slowly to ca. 80%, as shown previously in Figure 2b. The *cis*-butoxy- α CHO polymerization rate decreases significantly after 1 h as the $T_{\rm g}$ of the polymer approaches the reaction temperature. As both *cis*- and *trans*-butoxy- α CHO polymerizations reach conversions above ca. 70%, the reactions become increasingly limited by monomer diffusion to the active chain end rather than by the differences in reactivity between the two monomers.

These observations appear to be contradicted by the result that trans-bromo- α CHO is the most reactive monomer out of the α CHO series. However, the bromine substituent is significantly smaller than both the allyloxy and butoxy groups, and the steric contribution of this group is less significant than the CHO ether monomers. This result suggests that the size of the pendant group has a larger effect on polymerization kinetics than the relative position of the substituent when the group is directly adjacent to the epoxide. To better understand the differences in reactivity observed at the beginning of polymerization, DFT calculations were performed to extract relative intermediate state energies for the proposed polymerization mechanism for the different types of monomers.

Calculations of the Reaction Coordinate Diagram. In a previous study, we investigated a possible mechanism of a controlled epoxide ring-opening polymerization initiated by the MOBs. ⁸³ We observed that the polymerization proceeded after the in situ formation of a bisaluminum complex as the initiator. Inspired by this observation, here we propose a similar stepwise reaction pathway for the initiation of CHO and CHO-derived monomers (see Figure 4).

The DFT calculations were performed on Gaussian 16. The molecular geometry of each molecule and states 1, 2, 3, and 4 as well as the TS in the polymerization was optimized using the B3LYP functional with polarized plus diffusion 6-31+G** basis sets for all atoms and the Grimme D3 dispersion correction. The TSs were obtained using QST3 calculations and optimized until a single negative vibrational frequency was obtained (cf. Table S1). Benzyl groups on the nitrogen atoms were replaced with methyl groups to simplify the calculation. The initiation reaction pathway started with the monomer approaching the initiator and forming a coordination bond between the epoxide oxygen and the aluminum center (state

1). At this stage, the bicyclic monomer contained a cyclohexane ring with additional strain compared to the relaxed chair conformation. The twisted chair conformation has been previously reported for cyclohexene, where, similar to CHO, the ring is locked out of the preferred chair conformation, increasing the overall ring strain.84 This coordinated state exists in an equilibrium with uncoordinated monomer, and the relative energy difference between the uncoordinated and coordinated states correlates to the relative population of monomers coordinated to aluminum atoms. Subsequently, the four-membered ring in the bisaluminum complex opens to accommodate the monomer (state 2) and forms a six-membered ring TS where a nucleophilic substitution occurs that results in the enthalpy-driven ring opening of the epoxide (state 3). In state 4, the 2-(dimethylamino)ethoxyl group is attached to the ring-opened monomer, and a new four-membered-ring bisaluminum complex forms at the resting-state chain end for propagation. The transition from state 3 to state 4 also coincides with a conformational change in the cyclohexane ring from a twist chair to a chair, providing additional thermodynamic driving force for the reaction. Relative intermediate state and TS energies for the different monomers are enumerated in Table S2 in the Supporting Information. Dative bond lengths were typically longer for the α CHO series than the β CHO series, CHO, and the conventional epoxides. Additionally, all CHO monomers had lower overall ΔG^{\dagger} from their ground states to the rate limiting TS than the mono- and non-bicyclic disubstituted epoxides, indicating a lower kinetic barrier to polymerization for the CHO derivatives.

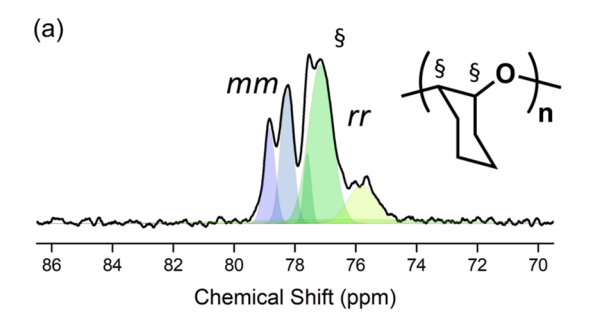
The lower activation barrier and greater thermodynamic driving force for CHO and CHO derivatives is assisted by a higher electron density on the epoxide oxygen than the terminal epoxide monomers. This result is consistent with the previous results by Hansen et al. who found that the increased electron density on the oxygen atom decreased the steric repulsion between the incoming nucleophile and the filled orbitals of the epoxide.⁷¹ Therefore, CHO is expected to be more Lewis basic with more electrophilic carbon atoms in the epoxide ring than terminal epoxides. It is also worth highlighting that the conformation of cyclohexane changed to the most stable "chair" conformation at state 4 from the twist-chair at state 3. Such a conformation change releases additional enthalpy for the polymerization of CHO and other bicyclic CHO-derived monomers compared to non-bicyclic epoxides such as propylene oxide and cis-2,3-butene oxide. Therefore, we propose that the high reactivity of CHO is attributed to its increased nucleophilicity, lower activation energy at the rate determining step, and its conformation change during the ring-opening process. Considering that this conclusion was drawn based on the calculation of electronic structure and the analysis of molecular geometry changes of CHO, it should be general and applicable to other Lewis acidcatalyzed ring-opening polymerizations and not just the MOB system reported here.

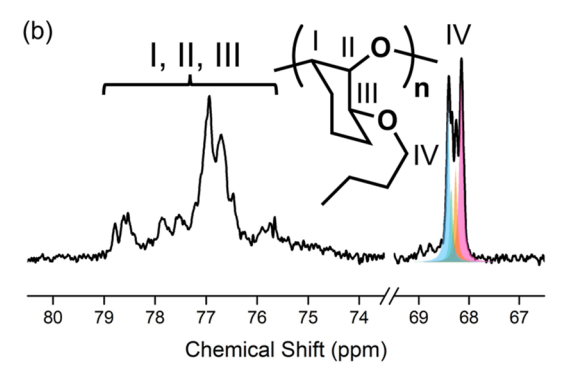
To better understand the differences in reactivity between the α CHO and β CHO series, CHO, *cis*-butoxy- α CHO, and *cis*-butoxy- β CHO can be compared. The change in Gibbs free energy to reach the TS (ΔG^{\ddagger}) was calculated to be ca. 32, 40, and 31 kcal/mol, respectively, for each monomer. The significantly higher ΔG^{\ddagger} of *cis*-butoxy- α CHO is likely caused by the stronger steric repulsion between the *n*-butyl group and the catalytically active species, consistent with the observed

slowest polymerization kinetics. The steric repulsion is less consequential for the β CHO series because the substituent is further away from the epoxide oxygen, resulting in shorter dative bond lengths compared to the α CHO series. Further examination of molecular geometry at state 1 revealed that CHO formed a strong coordination bond with a bond length of 2.388 Å with the aluminum center, while the coordination bond lengths for *cis*-butoxy- α CHO and *cis*-butoxy- β CHO were around 3.37 and 2.90 Å respectively, suggesting much weaker coordination in their geometries with the β CHO monomer more closely associated with the aluminum atom. Such a significant discrepancy in the coordination bond length was attributed to both the higher electron density on the epoxide oxygen of CHO compared to the other functionalized monomers, as indicated by the Mulliken charge calculation results, and the increased steric hindrance caused by the nbutyl substituents. The polymerization of CHO and the β CHO monomers additionally produced a significantly higher exotherm (ca. 20 kcal/mol) compared to α CHO (ca. 11–15 kcal/mol), which likely increased the rates of polymerization of the β CHO monomers relative to the α CHO monomers.

Regio- and Stereochemistry. ¹³C NMR spectroscopy was used to probe the regiochemical makeup of the resultant PCHOs. CHO polymerizes with little stereochemical regularity with achiral catalysts (see Figure 5a with peak assignments previously reported 35,36,72). We hypothesized that the α CHO series with pendant groups directly adjacent to the epoxide ring might limit the configurational degrees of freedom for addition to the growing polymer chain. Interestingly, as can be seen in Figure 5b, the polymerization of *cis*-butyl- α CHO produced a polymer with broad peaks possibly corresponding to isotactic, syndiotactic, and atactic sequences in the polymer. The overlapping signals between 68 and 68.6 ppm correspond to the ether carbon of the butyl group. The observed array of signals revealed that the polymer was likely composed of different constitutional regioisomers with the monomers adding with head-to-head, head-to-tail, tail-to-head, and tailto-tail linkages. This was also consistent with the increased number of peaks between 75 and 79 ppm. We hypothesize that this may be the case if the coordination step (state 1) of the mechanism does not favor aligning either of the electrophilic carbon atoms of the epoxide ring or either isomer of the CHO monomer prior to the ring-opening step. This is more likely in the β CHO series monomers than the α CHO series monomers because the substituent is further away from the epoxide oxygen in the β CHO series monomers and, therefore, likely has less directing influence. If the approach of the next monomer determines which carbon atom the alkoxide attacks and the coordination does not have a large energetic driving force to favor one orientation of the monomer over the other, a mixture of syndiotactic, isotactic, and atactic triads in the polymer with different constitutional isomers would be expected. Definitive assignments of these peaks, as well as the polyether backbone carbon peaks, are beyond the scope of this work and should be addressed in a future study.

For poly(butoxy- β CHO), the polyether backbone carbon peaks are significantly broader and less well defined than PCHO and poly(*cis*-butoxy- α CHO). The plurality of signals observed at ca. 68 ppm in Figure 5b corresponding to different constitutional isomers is not present in the peak at 71.2 ppm in Figure 5c. Because the butyl group is farther away from the stereocenters along the polymer backbone, it is likely that the signal for this carbon is less influenced by the regio- and





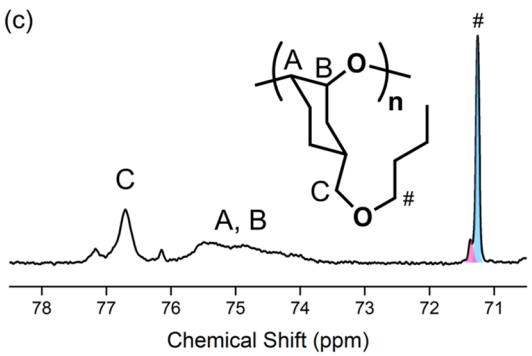


Figure 5. ¹³C NMR spectroscopy (CD₂Cl₂, 500 MHz) of (a) PCHO, (b) poly(cis-butoxy-αCHO), and (c) poly(butoxy-βCHO). Peak assignments for (a) have previously been reported in the literature while the assignments for (b,c) are based on HSQC (Figures S60 and S61 in the Supporting Information). Deconvolution was done using MATLAB with arbitrary peak colors used.

stereochemistry of the backbone. Nevertheless, the broadness of the peak corresponding to carbons A and B of this polymer are likely caused by a mixture of atactic, isotactic, and syndiotactic triads along the backbone as well as constitutional isomers. These results, in conjunction with the modeling results, indicate that the polymerization of CHO with an achiral catalyst does not produce polymers with large degrees of regioregularity. The polymerization can occur at either of the tertiary carbon atoms of the epoxide ring. Although the substituents on the α position to the epoxide ring significantly reduce the polymerization rates of α CHO monomers, the CHO unit's high reactivity reduces pendant group's ability to fully control the orientation in which monomers are added to the growing polymer chains.

Thermal Properties of Substituted Poly(CHO)s. Glass transition temperature was determined for each polymer using differential scanning calorimetry (DSC). Most polyethers have $T_{\rm g}$ s well below 0 °C (See Table 1) and are, therefore, viscous liquids at room temperature. One attractive quality of PCHO is its higher glass transition temperature of ca. 60 °C. The

substituted PCHOs all share the poly(CHO) backbone, and were, therefore, expected to have significantly higher T_g s than the analogous glycidyl ethers. All $P(\alpha CHO)$ s had glass transition temperatures above 0 °C. Poly(cis-allyloxy- α CHO), with the allyl pendant group *cis* to the epoxide, had a T_g ca. 30 °C, while poly(cis-butoxy- α CHO), with the butyl group cis to the epoxide, had a T_g of ca. 15–16 °C; a difference that may originate from the relative size of the pendant groups. The butyl group is larger and has more free rotation than the allyl group, which may facilitate increased relative segmental motion. Interestingly, when the butyl group is in the trans position relative to the epoxide ring, the $T_{\rm g}$ increases to ca. 35 °C, indicating more hindered relative segmental motion. Poly(allyloxy- β CHO) had a $T_{\rm g}$ ca. -11 °C and poly(butoxy- β CHO) had a $T_{\rm g}$ ca. -19 °C. The $T_{\rm g}$ for both PCHOs are significantly lower than their α CHO counterparts, but still well above that of the corresponding glycidyl ethers. The likely reason for this drop in $T_{\rm g}$ compared to the α CHO counterparts is that these polymers have longer side chains that are farther away from the polymer backbone, and this difference in position relative to the backbone could lead to an increase in polymer chain spacing.

In contrast to the other substituted PCHOs, the halogenated PCHOs, which have smaller pendant groups than the allyl and *n*-butyl CHOs, formed glassy polymers with T_{σ} s significantly higher [ca. 25 °C higher for poly(chloro-βCHO) and 50 °C higher for poly(trans-bromo- α CHO)] than unsubstituted PCHO. This result is consistent with the poly(glycidyl ether)s, where PECH has a significantly higher T_g than PnBGE and PAGE. The P(α CHO) $T_{\rm g}$ being higher than the analogous $P(\beta CHO)$ T_g is consistent with the results for the allyl and nbutyl substituted PCHOs. Although these $P(\alpha CHO)$ polymers have their substituents in different positions relative to the epoxide ring, they all have $T_{\rm g}$ s significantly above that of the analogous $P(\beta CHO)$, suggesting that it is not just the stereochemistry of the substitution relative to the epoxide that affects the glass transition temperature. It is likely that the steric bulk of the substituent and how the substituent impacts the polymer chain's ability to pack together and resist relative segmental motion have the greatest effect on the glass transition temperature. Figure 6 shows the effect of the butyl substituent's placement on the resulting polymer T_g .

CONCLUSIONS

We report the synthesis and characterization of new polymers made from functionalized CHOs. Kinetic studies reveal the rate of polymerization had a strong dependence on both the type of substituent present in the monomer as well as the position of the substituent relative to the epoxide ring. The variability in polymerization kinetics motivated DFT calculations to investigate a possible mechanism for the polymerization by analyzing intermediate and TS energies of the polymerization initiation event. Our computational work suggested that CHO's high reactivity relative to other epoxide monomers is due to its improved ability to coordinate to Lewis acids relative to other epoxides. Additional polymerization driving force comes from the release of ring strain caused by the opening of the epoxide ring and subsequent cyclohexane ring conversion to a more stable chair conformation from a higher-strain twist-chair. The scope of new materials and methods expand the range of polyethers available with a rigid poly(CHO) backbone and create a synthetic platform that can be expanded to a range of CHO-based monomers analogous to

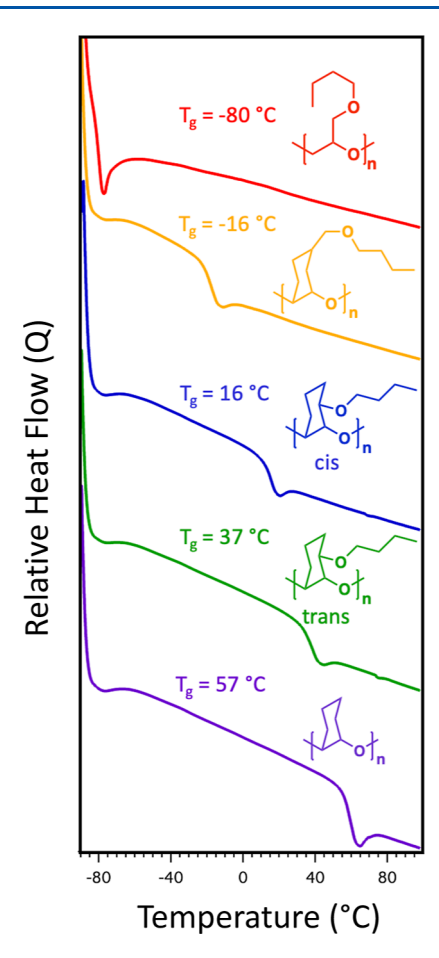


Figure 6. DSC traces of P(nBGE) (red), poly(butoxy-βCHO) (yellow), poly(cis-butoxy-αCHO) (blue), poly(trans-butoxy-αCHO) (green), and pCHO (purple).

the vast library of mono-substituted epoxide monomers. The resultant materials will likely have significantly higher glass transition temperatures than analogous polyethers with a poly(ethylene oxide)-based backbone and, therefore, may find uses in applications where a high $T_{\rm g}$ is desired.

ASSOCIATED CONTENT

Supporting Information

The Supporting Information is available free of charge at https://pubs.acs.org/doi/10.1021/acs.macromol.3c00473.

Experimental/computation details and molecular/thermal characterization data including ¹H NMR spectroscopy, ¹³C NMR spectroscopy, size exclusion chromatography, and DSC (PDF)

AUTHOR INFORMATION

Corresponding Author

Nathaniel A. Lynd — McKetta Department of Chemical Engineering and Texas Materials Institute, The University of Texas at Austin, Austin, Texas 78712, United States; orcid.org/0000-0003-3010-5068; Email: lynd@che.utexas.edu

Authors

Benjamin J. Pedretti — McKetta Department of Chemical Engineering, The University of Texas at Austin, Austin, Texas 78712, United States; orcid.org/0000-0003-2461-822X

Congzhi Zhu — McKetta Department of Chemical Engineering, The University of Texas at Austin, Austin, Texas 78712, United States; orcid.org/0000-0002-1302-7187

Hironobu Watanabe — Department of Macromolecular Science, Graduate School of Science, Osaka University, Osaka 560-0043, Japan; Present Address: Graduate School of Engineering Molecular and Macromolecular Chemistry, Nagoya University, Chikusa-ku, Nagoya 464-8601, Japan; orcid.org/0000-0002-0911-8836

Sadahito Aoshima — Department of Macromolecular Science, Graduate School of Science, Osaka University, Osaka 560-0043, Japan; oorcid.org/0000-0002-7353-9272

Complete contact information is available at: https://pubs.acs.org/10.1021/acs.macromol.3c00473

Notes

The authors declare no competing financial interest.

ACKNOWLEDGMENTS

This work was supported in part by a grant from the Robert A. Welch Foundation under grant no. F-1904 (C.Z. and N.A.L., characterization and materials and supplies support); the National Science Foundation under grant no. CHE-2004167 (B.J.P. and N.A.L., synthesis, stipend support, and characterization); and the Center for Materials for Water and Energy Systems (M-WET), an Energy Frontier Research Center funded by the U.S. Department of Energy, Office of Science, Basic Energy Sciences under award # DE-SC0019272 (B.J.P. and N.A.L., synthesis, stipend support, and characterization).

REFERENCES

- (1) He, J.; Ling, J.; Chiu, P. Vinyl Epoxides in Organic Synthesis. *Chem. Rev.* **2014**, *114*, 8037–8128.
- (2) Aziridines and Epoxides in Organic Synthesis, 1st ed.; Yudin, A., Ed.; Wiley-VCH Verlag GmbH & Co., 2006.
- (3) Smith, J. G. Synthetically Usefuly Reactions of Epoxides. *Synthesis* **1984**, 1984, 629–656.
- (4) Shukla, G.; Ferrier, R. C. The Versatile, Functional Polyether, Polyepichlorohydrin: History, Synthesis, and Applications. *J. Polym. Sci.* **2021**, *59*, 2704–2718.
- (5) Isono, T. Synthesis of Functional and Architectural Polyethers via the Anionic Ring-Opening Polymerization of Epoxide Monomers Using a Phosphazene Base Catalyst. *Polym. J.* **2021**, *53*, 753–764.
- (6) Childers, M. I.; Longo, J. M.; Van Zee, N. J.; LaPointe, A. M.; Coates, G. W. Stereoselective Epoxide Polymerization and Copolymerization. *Chem. Rev.* **2014**, *114*, 8129–8152.
- (7) Nakano, K.; Nozaki, K.; Hiyama, T. Asymmetric Alternating Copolymerization of Cyclohexene Oxide and CO ₂ with Dimeric Zinc Complexes. *J. Am. Chem. Soc.* **2003**, *125*, 5501–5510.
- (8) Trott, G.; Saini, P. K.; Williams, C. K. Catalysts for CO ₂/ Epoxide Ring-Opening Copolymerization. *Philos. Trans. R. Soc., A* **2016**, *374*, 20150085.
- (9) Kember, M. R.; Copley, J.; Buchard, A.; Williams, C. K. Triblock Copolymers from Lactide and Telechelic Poly(Cyclohexene Carbonate). *Polym. Chem.* **2012**, *3*, 1196–1201.
- (10) Herzberger, J.; Frey, H. E. Epicyanohydrin: Polymerization by Monomer Activation Gives Access to Nitrile-Amino-and Carboxyl-Functional Poly(ethylene glycol). *Macromolecules* **2015**, *48*, 8144–8153.
- (11) Herzberger, J.; Niederer, K.; Pohlit, H.; Seiwert, J.; Worm, M.; Wurm, F. R.; Frey, H. Polymerization of Ethylene Oxide, Propylene Oxide, and Other Alkylene Oxides: Synthesis, Novel Polymer Architectures, and Bioconjugation. *Chem. Rev.* **2016**, *116*, 2170–2243.
- (12) Patterson, A. L.; Wenning, B.; Rizis, G.; Calabrese, D. R.; Finlay, J. A.; Franco, S. C.; Zuckermann, R. N.; Clare, A. S.; Kramer,

- E. J.; Ober, C. K.; Segalman, R. A. Role of Backbone Chemistry and Monomer Sequence in Amphiphilic Oligopeptide- and Oligopeptoid-Functionalized PDMS- and PEO-Based Block Copolymers for Marine Antifouling and Fouling Release Coatings. *Macromolecules* **2017**, *50*, 2656–2667.
- (13) Lee, B. F.; Kade, M. J.; Chute, J. A.; Gupta, N.; Campos, L. M.; Fredrickson, G. H.; Kramer, E. J.; Lynd, N. A.; Hawker, C. J. Poly(Allyl Glycidyl Ether)-A Versatile and Functional Polyether Platform. *J. Polym. Sci., Part A* **2011**, *49*, 4498–4504.
- (14) Obermeier, B.; Frey, H. Poly(Ethylene Glycol- *Co* -Allyl Glycidyl Ether)s: A PEG-Based Modular Synthetic Platform for Multiple Bioconjugation. *Bioconjugate Chem.* **2011**, *22*, 436–444.
- (15) Liu, T.; Geng, X.; Nie, Y.; Chen, R.; Meng, Y.; Li, X. Hyperbranched Polyethers with Tunable Glass Transition Temperature: Controlled Synthesis and Mixing Rules. *RSC Adv.* **2014**, *4*, 30250–30258.
- (16) Ferrier, R. C.; Imbrogno, J.; Rodriguez, C. G.; Chwatko, M.; Meyer, P. W.; Lynd, N. A. Four-Fold Increase in Epoxide Polymerization Rate with Change of Alkyl-Substitution on Mono-μ-Oxo-Dialuminum Initiators. *Polym. Chem.* **2017**, *8*, 4503–4511.
- (17) Brocas, A.-L.; Mantzaridis, C.; Tunc, D.; Carlotti, S. Polyether Synthesis: From Activated or Metal-Free Anionic Ring-Opening Polymerization of Epoxides to Functionalization. *Prog. Polym. Sci.* **2013**, *38*, 845–873.
- (18) Parker, R. E.; Isaacs, N. S. Mechanisms Of Epoxide Reactions. *Chem. Rev.* **1959**, *59*, 737–799.
- (19) Barteau, K. P.; Wolffs, M.; Lynd, N. A.; Fredrickson, G. H.; Kramer, E. J.; Hawker, C. J. Allyl Glycidyl Ether-Based Polymer Electrolytes for Room Temperature Lithium Batteries. *Macromolecules* **2013**, *46*, 8988–8994.
- (20) Bulut, U.; Crivello, J. V. Investigation of the Reactivity of Epoxide Monomers in Photoinitiated Cationic Polymerization. *Macromolecules* **2005**, *38*, 3584–3595.
- (21) Crivello, J. V. A. New Visible Light Sensitive Photoinitiator System for the Cationic Polymerization of Epoxides: Light Sensitive Photoinitiator System. *J. Polym. Sci., Part A* **2009**, *47*, 866–875.
- (22) Sangermano, M.; Rodriguez, D.; Gonzalez, M. C.; Laurenti, E.; Yagci, Y. Visible Light Induced Cationic Polymerization of Epoxides by Using Multiwalled Carbon Nanotubes. *Macromol. Rapid Commun.* **2018**, *39*, 1800250.
- (23) Labbé, A.; Carlotti, S.; Billouard, C.; Desbois, P.; Deffieux, A. Controlled High-Speed Anionic Polymerization of Propylene Oxide Initiated by Onium Salts in the Presence of Triisobutylaluminum. *Macromolecules* **2007**, *40*, 7842–7847.
- (24) Rodriguez, C. G.; Ferrier, R. C.; Helenic, A.; Lynd, N. A. Ring-Opening Polymerization of Epoxides: Facile Pathway to Functional Polyethers via a Versatile Organoaluminum Initiator. *Macromolecules* **2017**, *50*, 3121–3130.
- (25) Widger, P. C. B.; Ahmed, S. M.; Coates, G. W. Exploration of Cocatalyst Effects on a Bimetallic Cobalt Catalyst System: Enhanced Activity and Enantioselectivity in Epoxide Polymerization. *Macromolecules* **2011**, *44*, 5666–5670.
- (26) Hirahata, W.; Thomas, R. M.; Lobkovsky, E. B.; Coates, G. W. Enantioselective Polymerization of Epoxides: A Highly Active and Selective Catalyst for the Preparation of Stereoregular Polyethers and Enantiopure Epoxides. J. Am. Chem. Soc. 2008, 130, 17658–17659.
- (27) Cong, K.; Liu, Z.; He, J.; Yang, R. Preparation and Performance of Polyether Elastomer with a Combination of Polyurethane and Polytriazole. *J. Appl. Polym. Sci.* **2022**, *139*, 51842.
- (28) Lan, P. N.; Corneillie, S.; Schacht, E.; Davies', M.; Shard, A. Synthesis and characterization of segmented polyurethanes based on amphiphilic polyether diols. *Biomaterials* **1996**, *17*, 2273–2280.
- (29) Miller, J. A.; Lin, S. B.; Hwang, K. K. S.; Wu, K. S.; Gibson, P. E.; Cooper, S. L. Properties of Polyether-Polyurethane Block Copolymers: Effects of Hard Segment Length Distribution. *Macromolecules* 1985, 18, 32–44.
- (30) Qu, Z.; Zhai, J.; Yang, R. Comparison between Properties of Polyether Polytriazole Elastomers and Polyether Polyurethane

- Elastomers: Properties Comparison between Polyurethane and Polytriazole Elastomers. *Polym. Adv. Technol.* **2014**, 25, 314–321.
- (31) Vandenberg, E. J. Some Aspects of the Bimetallic μ -Oxo-Alkoxides for Polymerizing Epoxides to Polyether Elastomers. *J. Polym. Sci., Polym. Chem.* **1986**, 24, 1423–1431.
- (32) Vandenberg, E. J. Organometallic Catalysts for Polymerizing Monosubstituted Epoxides. *J. Polym. Sci.* **1960**, 47, 486–489.
- (33) Vandenberg, E. J. Epoxide Polymers: Synthesis, Stereochemistry, Structure, and Mechanism. *J. Polym. Sci., Part A* **1969**, 7, 525–567.
- (34) Vandenberg, E. J. High Polymers from Symmetrical Disubstituted Epoxides. *J. Polym. Sci.* **1960**, 47, 489–491.
- (35) Sepulchre, M.; Kassamaly, A.; Spassky, N. Stereospecific Polymerization of Cyclohexene Oxide. *Makromol. Chem., Macromol. Symp.* **1991**, 42–43, 489–500.
- (36) Hasebe, Y.; Izumitani, K.; Torii, M.; Tsuruta, T. Studies on Elementary Reactions in the Polymerization of 1,2-Epoxycyclohexane with Organozim Compounds as Initiators. *Makromol. Chem.* **1990**, 191, 107–119.
- (37) Bentley, C. L.; Song, T.; Pedretti, B. J.; Lubben, M. J.; Lynd, N. A.; Brennecke, J. F. Effects of Poly(Glycidyl Ether) Structure and Ether Oxygen Placement on CO $_2$ Solubility. *J. Chem. Eng. Data* **2021**, *66*, 2832–2843.
- (38) Singh, G. S.; Mollet, K.; D'hooghe, M.; De Kimpe, N. Epihalohydrins in Organic Synthesis. *Chem. Rev.* **2013**, *113*, 1441–1408
- (39) Buchard, A.; Jutz, F.; Kember, M. R.; White, A. J. P.; Rzepa, H. S.; Williams, C. K. Experimental and Computational Investigation of the Mechanism of Carbon Dioxide/Cyclohexene Oxide Copolymerization Using a Dizinc Catalyst. *Macromolecules* **2012**, *45*, 6781–6795.
- (40) Kember, M. R.; White, A. J. P.; Williams, C. K. Di- and Tri-Zinc Catalysts for the Low-Pressure Copolymerization of CO ₂ and Cyclohexene Oxide. *Inorg. Chem.* **2009**, *48*, 9535–9542.
- (41) Kember, M. R.; White, A. J. P.; Williams, C. K. Highly Active Di- and Trimetallic Cobalt Catalysts for the Copolymerization of CHO and CO ₂ at Atmospheric Pressure. *Macromolecules* **2010**, *43*, 2291–2298.
- (42) Jutz, F.; Buchard, A.; Kember, M. R.; Fredriksen, S. B.; Williams, C. K. Mechanistic Investigation and Reaction Kinetics of the Low-Pressure Copolymerization of Cyclohexene Oxide and Carbon Dioxide Catalyzed by a Dizinc Complex. *J. Am. Chem. Soc.* **2011**, *133*, 17395–17405.
- (43) Cohen, C. T.; Thomas, C. M.; Peretti, K. L.; Lobkovsky, E. B.; Coates, G. W. Copolymerization of Cyclohexene Oxide and Carbon Dioxide Using (Salen)Co(III) Complexes: Synthesis and Characterization of Syndiotactic Poly(Cyclohexene Carbonate). *Dalton Trans.* **2006**, *1*, 237–249.
- (44) Reis, N. V.; Deacy, A. C.; Rosetto, G.; Durr, C. B.; Williams, C. K. Heterodinuclear Mg(II)M(II) (M=Cr, M_n, Fe, Co, Ni, Cu and Zn) Complexes for the Ring Opening Copolymerization of Carbon Dioxide/Epoxide and Anhydride/Epoxide. *Chem.—Eur. J.* **2022**, 28, No. e202104198.
- (45) Li, W.-B.; Liu, Y.; Lu, X.-B. Bimetallic Cobalt Complex-Mediated Enantioselective Terpolymerizations of Carbon Dioxide, Cyclohexene Oxide, and β -Butyrolactone. *Organometallics* **2020**, 39, 1628–1633.
- (46) Scharfenberg, M.; Hofmann, S.; Preis, J.; Hilf, J.; Frey, H. Rigid Hyperbranched Polycarbonate Polyols from CO ₂ and Cyclohexene-Based Epoxides. *Macromolecules* **2017**, *50*, 6088–6097.
- (47) Koning, C.; Wildeson, J.; Parton, R.; Plum, B.; Steeman, P.; Darensbourg, D. J. Synthesis and Physical Characterization of Poly(Cyclohexane Carbonate), Synthesized from CO2 and Cyclohexene Oxide. *Polymer* **2001**, *42*, 3995–4004.
- (48) Biernesser, A. B.; Delle Chiaie, K. R.; Curley, J. B.; Byers, J. A. Block Copolymerization of Lactide and an Epoxide Facilitated by a Redox Switchable Iron-Based Catalyst. *Angew. Chem., Int. Ed.* **2016**, *55*, 5251–5254.

- (49) Qi, M.; Dong, Q.; Wang, D.; Byers, J. A. Electrochemically Switchable Ring-Opening Polymerization of Lactide and Cyclohexene Oxide. J. Am. Chem. Soc. 2018, 140, 5686–5690.
- (50) Quan, S. M.; Wei, J.; Diaconescu, P. L. Mechanistic Studies of Redox-Switchable Copolymerization of Lactide and Cyclohexene Oxide by a Zirconium Complex. *Organometallics* **2017**, *36*, 4451–4457.
- (51) Han, B.; Zhang, L.; Liu, B.; Dong, X.; Kim, I.; Duan, Z.; Theato, P. Controllable Synthesis of Stereoregular Polyesters by Organocatalytic Alternating Copolymerizations of Cyclohexene Oxide and Norbornene Anhydrides. *Macromolecules* **2015**, *48*, 3431–3437.
- (52) Romain, C.; Zhu, Y.; Dingwall, P.; Paul, S.; Rzepa, H. S.; Buchard, A.; Williams, C. K. Chemoselective Polymerizations from Mixtures of Epoxide, Lactone, Anhydride, and Carbon Dioxide. *J. Am. Chem. Soc.* **2016**, *138*, 4120–4131.
- (53) Saini, P. K.; Romain, C.; Zhu, Y.; Williams, C. K. Di-Magnesium and Zinc Catalysts for the Copolymerization of Phthalic Anhydride and Cyclohexene Oxide. *Polym. Chem.* **2014**, *5*, 6068–6075.
- (54) Sanford, M. J.; Peña Carrodeguas, L.; Van Zee, N. J.; Kleij, A. W.; Coates, G. W. Alternating Copolymerization of Propylene Oxide and Cyclohexene Oxide with Tricyclic Anhydrides: Access to Partially Renewable Aliphatic Polyesters with High Glass Transition Temperatures. *Macromolecules* **2016**, *49*, 6394–6400.
- (55) Hosseini Nejad, E.; van Melis, C. G. W.; Vermeer, T. J.; Koning, C. E.; Duchateau, R. Alternating Ring-Opening Polymerization of Cyclohexene Oxide and Anhydrides: Effect of Catalyst, Cocatalyst, and Anhydride Structure. *Macromolecules* **2012**, *45*, 1770–1776.
- (56) Plajer, A. J.; Williams, C. K. Heterotrinuclear Ring Opening Copolymerization Catalysis: Structure—Activity Relationships. *ACS Catal.* **2021**, *11*, 14819—14828.
- (57) Gregory, G. L.; Williams, C. K. Exploiting Sodium Coordination in Alternating Monomer Sequences to Toughen Degradable Block Polyester Thermoplastic Elastomers. *Macromolecules* **2022**, *55*, 2290–2299.
- (58) Dai, R.; Diaconescu, P. L. Investigation of a Zirconium Compound for Redox Switchable Ring Opening Polymerization. *Dalton Trans.* **2019**, *48*, 2996–3002.
- (59) Hern, Z. C.; Quan, S. M.; Dai, R.; Lai, A.; Wang, Y.; Liu, C.; Diaconescu, P. L. ABC and ABAB Block Copolymers by Electrochemically Controlled Ring-Opening Polymerization. *J. Am. Chem. Soc.* **2021**, *143*, 19802–19808.
- (60) Quan, S. M.; Wang, X.; Zhang, R.; Diaconescu, P. L. Redox Switchable Copolymerization of Cyclic Esters and Epoxides by a Zirconium Complex. *Macromolecules* **2016**, 49, 6768–6778.
- (61) Wei, J.; Diaconescu, P. L. Redox-Switchable Ring-Opening Polymerization with Ferrocene Derivatives. *Acc. Chem. Res.* **2019**, *52*, 415–424.
- (62) Fan, H.; Yang, X.; Chen, J.; Tu, Y.; Cai, Z.; Zhu, J. Advancing the Development of Recyclable Aromatic Polyesters by Functionalization and Stereocomplexation. *Angew. Chem.* **2022**, *134*, No. e202117639.
- (63) Yang, X.; Zhang, W.; Huang, H.-Y.; Dai, J.; Wang, M.-Y.; Fan, H.-Z.; Cai, Z.; Zhang, Q.; Zhu, J.-B. Stereoselective Ring-Opening Polymerization of Lactones with a Fused Ring Leading to Semicrystalline Polyesters. *Macromolecules* **2022**, *55*, 2777–2786.
- (64) Li, Z.; Shen, Y.; Li, Z. Chemical Upcycling of Poly(3-Hydroxybutyrate) into Bicyclic Ether–Ester Monomers toward Value-Added, Degradable, and Recyclable Poly(Ether Ester). ACS Sustainable Chem. Eng. 2022, 10, 8228–8238.
- (65) Coates, G. W.; Getzler, Y. D. Y. L. Chemical Recycling to Monomer for an Ideal, Circular Polymer Economy. *Nat. Rev. Mater.* **2020**, *5*, 501–516.
- (66) Singer, F. N.; Deacy, A. C.; McGuire, T. M.; Williams, C. K.; Buchard, A. Chemical Recycling of Poly(Cyclohexene Carbonate) Using a Di-Mg ^{II} Catalyst. *Angew. Chem., Int. Ed.* **2022**, *61*, No. e202201785.

- (67) Ambrose, K.; Murphy, J. N.; Kozak, C. M. Chromium Amino-Bis(Phenolate) Complexes as Catalysts for Ring-Opening Polymerization of Cyclohexene Oxide. *Macromolecules* **2019**, *52*, 7403–7412.
- (68) Inoue, M.; Kanazawa, A.; Aoshima, S. Living Cationic Ring-Opening Homo- and Copolymerization of Cyclohexene Oxide by "Dormant" Species Generation Using Cyclic Ethers as Lewis Basic Additives. *Macromolecules* **2021**, *54*, 5124–5135.
- (69) Plommer, H.; Reim, I.; Kerton, F. M. Ring-Opening Polymerization of Cyclohexene Oxide Using Aluminum Amine—Phenolate Complexes. *Dalton Trans.* **2015**, *44*, 12098—12102.
- (70) Schneiderman, D. K.; Hillmyer, M. A. Aliphatic Polyester Block Polymer Design. *Macromolecules* **2016**, *49*, 2419–2428.
- (71) Hansen, T.; Vermeeren, P.; Yoshisada, R.; Filippov, D. V.; van der Marel, G. A.; Codée, J. D. C.; Hamlin, T. A. How Lewis Acids Catalyze Ring-Openings of Cyclohexene Oxide. *J. Org. Chem.* **2021**, *86*, 3565–3573.
- (72) Hasebe, Y.; Tsuruta, T. Structural Studies of Poly(1 ,2-Cyclohexene Oxide) Prepared with Well-Defined Organozinc Compounds. *Makromol. Chem.* **1987**, *188*, 1403–1414.
- (73) Freccero, M.; Gandolfi, R.; Sarzi-Amadè, M.; Rastelli, A. Facial Selectivity in Epoxidation of 2-Cyclohexen-1-Ol with Peroxy Acids. A Computational DFT Study. *J. Org. Chem.* **2000**, *65*, 8948–8959.
- (74) Denton, R. M.; An, J.; Adeniran, B.; Blake, A. J.; Lewis, W.; Poulton, A. M. Catalytic Phosphorus(V)-Mediated Nucleophilic Substitution Reactions: Development of a Catalytic Appel Reaction. *J. Org. Chem.* **2011**, *76*, 6749–6767.
- (75) Samek, Z.; Budesinsky, M. In Situ Reactions with Trichloroacetyl Isocyanate and Their Application to Structural Assignment of Hydroxy Compounds by 1H NMR Spectroscopy. A General Comment. Collect. Czech. Chem. Commun. 1979, 44, 558.
- (76) Fürst, A.; Plattner, Pl. A. Über Steroide und Sexualhormone. 160. Mitteilung. 2α , 3α und 2β , 3β -Oxido-chlolestane; Konfiguration der 2-Oxy-cholestane. *Helv. Chim. Acta* **1949**, 32, 275–283.
- (77) Chini, M.; Crotti, P.; Flippin, L. A.; Macchia, F. Regiochemical Control of the Ring-Opening of 1,2-Epoxides by Means of Chelating Processes. Synthesis and Reactions of the Cis- and Trans-Oxides Derived from 4-(Benzyloxy)Cyclohexene. *J. Org. Chem.* **1990**, *55*, 4265–4272.
- (78) Chini, M.; Crotti, P.; Flippin, L. A.; Macchia, F. Regiochemical Control of the Ring-Opening of 1,2-Epoxides by Means of Chelating Processes. 3. Aminolysis and Azidolysis of the Cis- and Trans-Oxides Derived from 4-(Benzyloxy)Cyclohexene. *J. Org. Chem.* **1991**, *56*, 7043–7048.
- (79) Chini, M.; Crotti, P.; Flippin, L. A.; Macchia, F.; Pineschi, M. Regiochemical Control of the Ring-Opening of 1,2-Epoxides by Means of Chelating Processes. 2. Synthesis and Reactions of the Cisand Trans-Oxides of 4-[(Benzyloxy)Methyl]Cyclohexene, 3-Cyclohexenemethanol, and Methyl 3-Cyclohexenecarboxylate. *J. Org. Chem.* 1992, 57, 1405–1412.
- (80) Chini, M.; Crotti, P.; Favero, L.; Macchia, F. Stereo- and Regioselective Metal Salt-Catalyzed Alkynylation of 1,2-Epoxides. *Tetrahedron Lett.* **1991**, 32, 6617–6620.
- (81) Chini, M.; Crotti, P.; Gardelli, C.; Macchia, F. Metal Salt-Promoted Alcoholysis of 1,2-Epoxides. *Synlett* **1992**, *1992*, *673*–*676*.
- (82) Duda, J. L. Molecular Diffusion in Polymeric Systems. *Pure Appl. Chem.* **1985**, *57*, 1681–1690.
- (83) Imbrogno, J.; Ferrier, R. C.; Wheatle, B. K.; Rose, M. J.; Lynd, N. A. Decoupling Catalysis and Chain-Growth Functions of Mono(μ-Alkoxo)Bis(Alkylaluminums) in Epoxide Polymerization: Emergence of the N–Al Adduct Catalyst. *ACS Catal.* **2018**, *8*, 8796–8803.
- (84) Ibberson, R. M.; Telling, M. T. F.; Parsons, S. Crystal Structures and Glassy Phase Transition Behavior of Cyclohexene. *Cryst. Growth Des.* **2008**, *8*, 512–518.